1

Thermal and Relaxation Properties of Food and Biopolymers with Emphasis on Water

Jan Swenson[1] *and Helén Jansson*[2]

[1] *Department of Physics, Chalmers University of Technology, Göteborg, Sweden*
[2] *Department of Civil and Environmental Engineering, Chalmers University of Technology, Göteborg, Sweden*

1.1 Introduction

Thermal and relaxation properties of food and biological materials can hardly be discussed without considering the role of the surrounding water. In fact, we would not even have living organisms or food without water. Biomolecules, such as proteins, nucleic acids, polysaccharides and other smaller molecules that make up living organisms, need water for their structure and function. The water determines their mobility, allows them to associate and dissociate, enables proton transfer, and facilitates a large number of biochemical processes (Franks *et al.* 1983; Luby-Phelps *et al.* 1988; Rupley *et al.* 1991; Zimmerman *et al.* 1993). Since the water molecules are small and fast moving compared to most biomolecules their presence tends to speed up the dynamics of the biomolecules. When this is the case, water is said to act as a plasticizer for the biomaterial. Generally, this plasticizing effect of water can be huge and decrease the glass transition temperature of food and biomaterials by more than 100 K (Jansson *et al.* 2005). The strong influence on the water content is also of high medical and industrial importance since drying of food and biomaterial can considerably increase the stability and storage time at a given temperature, by simply increasing the glass transition temperature to above the storage temperature (Levine *et al.* 1990). However, it should here be noted that water has a large tendency to form hydrogen bonds to other molecules, and this can give rise to "superstructural units", with an increased relaxation (Sjostrom *et al.* 2011), and/or an increased interaction between different biomolecules, leading to an antiplasticizing effect of the water. Although such antiplasticizing effects are fairly uncommon they can be strong (Sjostrom *et al.* 2011). Furthermore, as will be discussed in some detail in this chapter, water influences the dynamics of other glass forming materials very differently at low and very high water contents. This further implies that equations like the empirical Gordon-Taylor equation (Gordon *et al.* 1952) (Eq. 1.1), commonly used to predict the glass transition temperature over wide concentration ranges, cannot be used to estimate the glass transition temperature of pure water.

$$T_g = \frac{w_1 T_{g1} + k w_2 T_{g2}}{w_1 + k w_2} \tag{1.1}$$

Glass Transition and Phase Transitions in Food and Biological Materials, First Edition.
Edited by Jasim Ahmed, Mohammad Shafiur Rahman, and Yrjö H. Roos.

In this equation T_g denotes the glass transition temperature of a two-component mixture and the subscripts 1 and 2 denote the components 1 and 2, respectively. The weight fraction of the components is denoted by w, and k is a system-dependent constant.

Sugar and other carbohydrates are essential components in plants, fruits, vegetables and all living organisms, where they have structural, cryoprotective and metabolic roles (Mathews *et al.* 2000). The cryoprotective role of carbohydrates are also of importance for the food industry, where cooling and drying are frequently used methods for food storage (Levine *et al.* 1990). In addition, glassy carbohydrates are commonly used in the encapsulation and stabilization of labile food ingredients (Gunning *et al.* 1999) and pharmaceuticals (Shamblin *et al.* 1999). Since the properties of carbohydrates are strongly dependent on the water-rich environment in which they are generally working, also their cryoprotective properties are controlled by their water-dependent molecular dynamics at low temperatures around their glass transition.

The properties of carbohydrates and carbohydrate-rich food and biological materials are thus strongly dependent on the associated water. However, the influence of water is probably even larger for the dynamics and biological functions of proteins. A protein is inactive in its dehydrated state up to a hydration level h=0.2 (g of water)/(g of protein), whereas for full activity roughly the same mass of water as protein is required (Rupley *et al.* 1983; Frauenfelder *et al.* 1986). This importance of water has been supported by several experiments (Fenimore *et al.* 2004; Frauenfelder *et al.* 2009) and molecular dynamics (MD) simulation studies (Vitkup *et al.* 2000; Tarek *et al.* 2002), which have shown that the protein motions are mainly determined by the water dynamics. Hence, the protein motions, which, in turn, are necessary for the biological activity of the protein, are "slaved" (or "driven") by the water motions (Frauenfelder *et al.* 2009). This "slaving" does not mean that the time scale of a protein motion is the same as for its surrounding water, but that the relaxation times of the two processes show similar temperature dependences, that is, similar activation energies at a given temperature. It should here be pointed out that water does not show unique properties as a solvent in all aspects. Provided that the folded protein structure can be kept basically intact in the solvent, it is mainly the viscosity of the solvent that determines the biologically most important global protein fluctuations. This can be achieved in a solvent such as glycerol (Rariy *et al.* 1997), or even in an environment of a polymer surfactant (Gallat *et al.* 2012), but not in, for example, ordinary alcohols, which causes denaturation of the protein. However, due to the higher viscosity of, for example, glycerol compared to water the global protein fluctuations, and related biological activities, are slowed down. In fact, the accumulation of low molecular weight carbohydrates such as glycerol in the body is the reason for why, for instance, various types of tree frogs can survive in climates of longer times of subzero temperatures without cold- and freezing-induced damage by the stabilization of protein and protection of membranes (Goldstein *et al.* 2010; Rexer-Huber *et al.* 2011) (and references therein). However, water has, as mentioned above, other unique properties as a solvent, which implies that the water in our bodies cannot be completely replaced by another solvent, but this will not be further discussed in this chapter.

In this chapter we will not only discuss the slaving behaviour of protein dynamics, as mentioned above, but also discuss the currently debated (Doster *et al.* 1986; Sartor *et al.* 1994; Jansson *et al.* 2010; Jansson *et al.* 2011) origin and broadness of the calorimetric glass transition of protein systems. Further focus will be on the thermal and relaxation

properties of sugar solutions and sugar-rich materials like fruits and vegetables. As for the proteins, we will discuss their relaxation properties and the related calorimetric glass transition. Finally, we will show that the structural and dynamical properties of water in solutions are very different at low and high solute concentrations, and that this leads to a failure of the Gordon-Taylor equation (Gordon *et al.* 1952) at high water contents. Since calorimetric glass transitions and other thermal events, such as melting and crystallizations, are most directly measured by differential scanning calorimetry (DSC) and associated relaxation properties are easiest studied by broadband dielectric spectroscopy, experimental data from these two techniques will be presented and provide the base for our conclusions.

1.2 Glass Transition and Relaxation Dynamics of Sugar Solutions and Sugar-Rich Food

In general, it is complicated to determine the glass transition temperature (T_g) of aqueous solutions of higher water contents due to that crystallisation normally occurs at sub-zero temperatures. Even if the crystallisation temperature of water in general is substantially lowered by both the addition of solutes, like sugar molecules, and/or by using high cooling rates, crystallisation of bulk water and aqueous solutions of higher water contents will always occur in the temperature range 150–230 K (Sellberg *et al.* 2014). This region, which is visualized in Figure 1.1, is called the "No man's land" of water due to its inaccessibility in a non-crystalline state.

One way to overcome the problem to determine the glass transition temperature, and especially to study the properties of water and diluted aqueous solutions in the "No man's land", is to confine the liquids in porous materials or on surfaces. When water is confined, the water molecules are affected by surfaces, which will induce a layering effect (Antognozzi *et al.* 2001; Jensen *et al.* 2004). This in turn changes the orientation of adjacent water molecules in a way that depends on the chemical nature of the surface (i.e., whether the surface is hydrophilic or hydrophobic, or positively or negatively charged) (Jensen *et al.* 2004) (and references therein). This orientation will in turn affect the interaction between the water molecules and, as a result, reducing the probability of forming the network structure necessary for crystallization (Takahara *et al.* 1999; Ricci *et al.* 2000; Raviv *et al.* 2001; Rovere *et al.* 2003). This will be further discussed in Section 1.4 below.

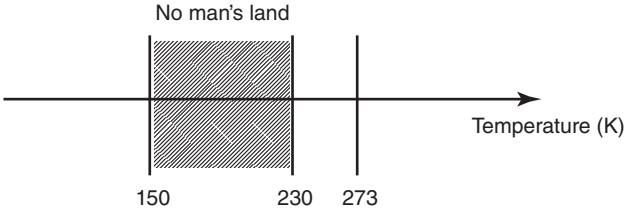

Figure 1.1 Schematic description of the so-called "No man's land" of water between 150 and 230 K. In this region crystallisation of bulk water and aqueous solutions of higher water contents cannot be avoided. 273 K is the melting temperature of bulk water.

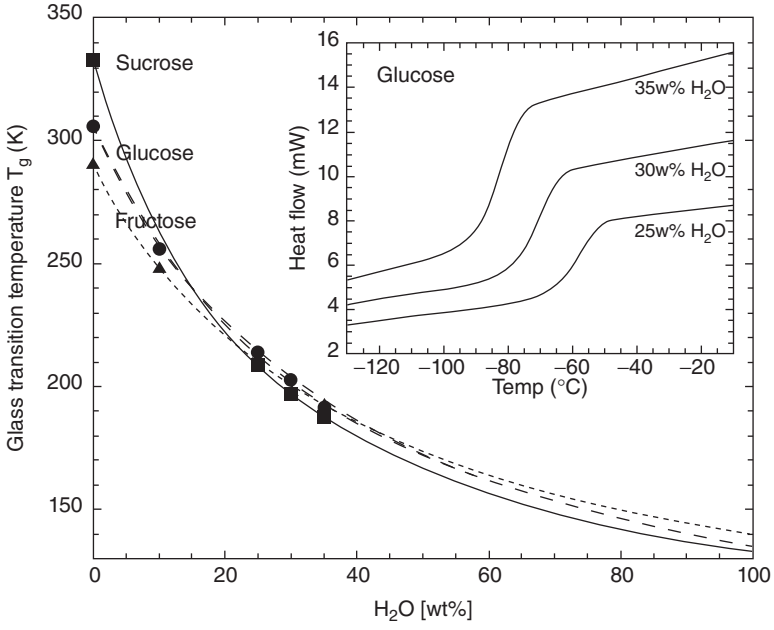

Figure 1.2 Gordon-Taylor plot of glass transition temperatures obtained from DSC measurements. The glass transition temperatures of the dry carbohydrates and carbohydrates with 10 wt% water content are taken from Fulcher *et al*. (Fulcher, 1925). The inset shows DSC data around the glass transition of glucose at the hydration levels 25, 30 and 35 wt% water. The glass transition temperature, T_g, was taken as the half step of the transition on cooling. The cooling rate for all measurements was 10 °C/min. The figure is taken from Jansson *et al*. (Jansson *et al.* 2005).

Another common way to determine the glass transition temperature of water-rich solutions is to determine T_g for the corresponding solutions of lower water contents, and then extrapolate it for solutions of higher water contents by use of its concentration dependence. Provided that the glass transition temperature of the aqueous solutions show a monotonic concentration dependence, the estimation is commonly done by the empirical Gordon Taylor (GT) equation (Eq. 1.1) (Gordon *et al.* 1952).

In the inset of Figure 1.2, the effect of the water content on the glass transition temperature is shown by the DSC thermograms for aqueous solutions of the monosaccharide glucose. As can be observed, T_g decreases with increasing water content. Thus indicating that water increases the mobility of the system and thus has a plasticizing effect on the sugar molecules. Furthermore, it is evident that the step in heat flow (which is proportional to the change in heat capacity) at the glass transition increases with increasing water concentration. The reason for this increase is probably an increase of the amplitude and/or in the cooperativity length (i.e., the number of molecules involved) of the motions associated with the viscosity. Both these scenarios are plausible due to the smaller size and larger density of hydrogen bonds of the water molecules, compared to the sugar molecules. On the other hand, if this increase of the step in heat flow is extrapolated to pure water it becomes considerably larger than the small calorimetric feature of hyperquenched bulk water at 136 K (Johari *et al.* 1987), which generally is accepted as the glass transition of water. In fact, the step in the heat capacity of bulk water

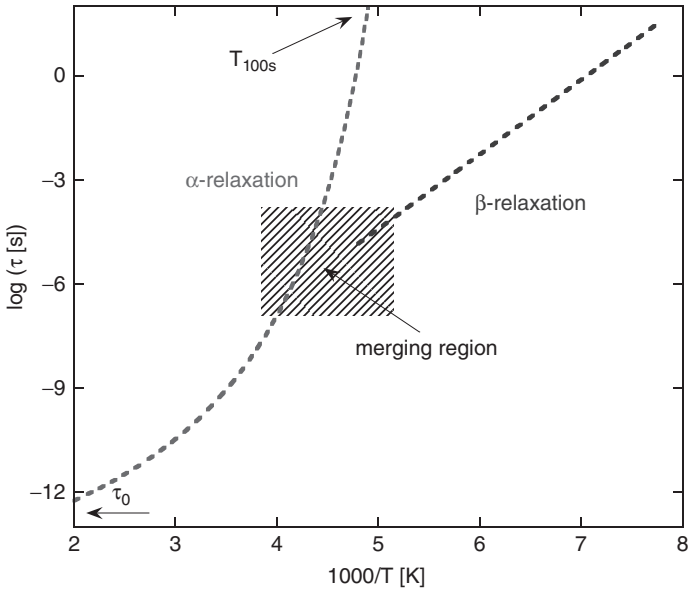

Figure 1.3 Schematic relaxation behaviour of a typical supercooled liquid. The relaxation process that is coupled to the macroscopic viscosity of the liquid is called the α-relaxation, which reaches a time scale of about 100 s at T_g. However, slightly above T_g, one or more local relaxation processes decouple from the structural α-relaxation. Such secondary relaxation processes are often denoted β-relaxations.

at 136 K is typically only 2% of what is commonly observed for the glass transition of aqueous solutions (Angell, 2008). This further questions whether the feature at 136 K can be associated with the freezing-in of the same type of molecular motions as in the case of the glass transition of aqueous solutions, particularly since no glass transition can be observed for confined water, in contrast to confined aqueous solutions, as will be discussed in Sections 1.3 and 1.4 below.

The glass transition of supercooled liquids can also be determined by the so-called α-relaxation, which is due to collective molecular rearrangements directly coupled to the macroscopic viscosity. As shown in the schematic illustration in Figure 1.3, the relaxation time (τ_α) of this process becomes increasingly slower with decreasing temperature. By definition, T_g is reached when τ_α reaches a value of about 100 s (in analogy with the 10^{13} poise $=10^{12}$ Nsm^{-2} for the viscosity). In addition to the structural α-relaxation, glass forming solutions generally also show weaker secondary relaxation processes, where the most common category are denoted β-relaxations. In aqueous solutions of higher water contents, the local process is usually dominated by the relaxation of water and therefore often called the w-relaxation. The β (or w-) relaxation is faster and of more local nature than the α-relaxation and it is visible also below T_g. As also visualized in this figure, the viscosity related (α) and the local (β or w) relaxations generally merge at a temperature somewhat above the glass transition temperature. Thus, at higher temperatures the two relaxation processes occur on the same time scale even if the viscosity-related relaxation dominates the spectrum.

The structural and viscosity related relaxation can easily be distinguished from the more local one by their different temperature behaviors, as shown in Figure 1.3. The

faster and more local β (or w) relaxation is normally described by the Arrhenius equation (Eq. 1.2), whereas the increase in relaxation time (or viscosity) with decreasing temperature of the α-relaxation generally follows a Vogel-Fulcher-Tammann behavior (Vogel, 1921; Fulcher, 1925; Tammann *et al.* 1926) (Eq. 1.3):

$$\tau = \tau_0 \exp(E_a/k_B T) \tag{1.2}$$

$$\tau = \tau_0 \exp\left(\frac{DT_0}{T - T_0}\right) \tag{1.3}$$

In these equations τ_0 is the microscopic relaxation time extrapolated to an infinite temperature, which usually corresponds to quasi-lattice and molecular vibrations of the order of 10^{-14} s. E_a is the activation energy, T_0 is the temperature where the relaxation time τ goes to infinity and D is a parameter that describes the deviation from Arrhenius behavior for the viscosity related α-relaxation. This D parameter is directly related to the so-called fragility of a glass forming liquid, where a strong deviation from an Arrhenius temperature dependence (i.e., a low values of D) of the α-relaxation means a fragile liquid and a nearly Arrhenius temperature dependence is a signature of a strong liquid (Angell, 1991). Fragile liquids are typically molecular systems with weak intermolecular interactions (e.g., Van der Waals), whereas strong liquids are often associated with a strong network structure of covalent bonds.

In Figure 1.4, the dielectric relaxation times for various sugar containing systems of 20 wt% water are shown. The slower cooperative and viscosity related α-relaxation of the whole system is shown by solid lines and the faster and more local water relaxation (w) by symbols. As can be observed, for the three sugar-based aqueous solutions (fructose, glucose and xylitol) the α-relaxation reaches a relaxation time of 100 s (T_{100s}), which, as mentioned above, is considered as the dielectric glass transition temperature, around 210 K, whereas it is found at a somewhat lower temperature (190 K) in case of hydrated strawberry. The faster and more local w-relaxation in the sugar based aqueous solutions can in principle be described by the Arrhenius equation in the entire temperature range for which it can be determined by certainty. However, due to that the extrapolated prefactor τ_0 is much lower than the typical molecular vibration time (typical around 10^{-14} s) this process much likely deviates from its Arrhenius temperature dependence at higher temperatures. This is in fact also what is observed for the strawberry sample. Here it should be noted that the strawberry sample does not correspond to fresh strawberry, but to a freeze-dried strawberry which has been hydrated to 20 wt% water in order to have the same water content as the sugar solutions shown in the same figure. In this material the w-relaxation follows an Arrhenius temperature dependence (Eq. 1.2) at low temperatures whereas at higher temperatures it is better described by the VFT equation (Eq. 1.3). As can be observed in Figure 1.4, for this specific sample the crossover in temperature dependence is found at about the same temperature as τ_α reaches 100 s. In fact, this crossover in temperature dependence from a low temperature Arrhenius behavior to a high temperature VFT dependence is commonly observed for water confined in a wide range of systems. It is observed in hard confining systems as well as on surfaces of soft biological materials, see for instance (Jansson *et al.* 2003; Swenson *et al.* 2006; Hedstrom *et al.* 2007; Monasterio *et al.* 2013; Swenson *et al.* 2015). The physical origin of this universal crossover in the water dynamics has been widely debated in recent years (Jansson *et al.* 2003). For instance, it has been suggested that supercooled water around biomolecules and in other types of confined geometries exhibits

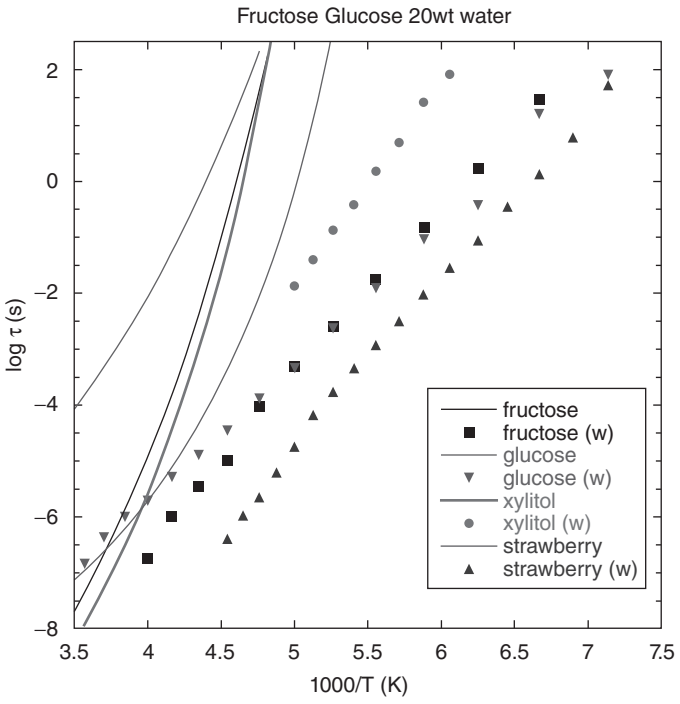

Figure 1.4 Dielectric relaxation times for the sugars fructose, glucose and xylitol containing 20 wt% water and freeze-dried strawberry at the same hydration level. The viscosity related α-relaxation of each system is given by solid lines and the more local water relaxation (w) is given by the symbols shown in the figure.

a liquid-liquid transition at a temperature of approximately 225 K (Faraone *et al.* 2004; Liu *et al.* 2005; Chen *et al.* 2006; Mallamace *et al.* 2006). Such a liquid-liquid transition would then also give rise to a crossover in the water dynamics, from a fragile (i.e., a pronounced non-Arrhenius temperature dependence of the viscosity and its related α-relaxation time) high temperature behaviour to a strong (i.e., an Arrhenius temperature dependence) low temperature behaviour (Faraone *et al.* 2004; Liu *et al.* 2005; Chen *et al.* 2006; Mallamace *et al.* 2006). It has also been suggested (Chen *et al.* 2006) that such a fragile-to-strong transition in the dynamics of the hydration water should lead to a similar transition of protein dynamics. However, we argued (Swenson *et al.* 2006) that no true fragile-to-strong transition is present for such hydration water, but that an apparent fragile-to-strong transition occurs where the merged high temperature $\alpha-\beta$ relaxation transforms to a local β-relaxation, as shown in Figure 1.3. This interpretation has recently been accepted (Wang *et al.* 2014) by several of the authors who proposed the presence of a true fragile-to-strong transition in the dynamics of confined and hydration water. Therefore, it can now be concluded that there are no experimental evidences for a true fragile-to-strong transition in the dynamics of hydration water, and this also questions the presence of a liquid-liquid transition in the hydration water around 225 K.

From Figure 1.4 it is also interesting to note that the dynamics in a real and complex system, like the hydrated strawberry material, is very similar to that of the sugar solutions. Both the large-scale α-relaxation and the more local relaxation (β or w) show

similar temperature behaviors. The reason for this is most likely that water molecules in the strawberry structure are mainly interacting with carbohydrates of different kinds. Furthermore, from the temperature dependence of the viscosity related α-relaxation (solid lines) it is evident that the dynamical properties of the strawberry matrix changes substantially with temperature. At low temperatures the matrix can be considered as rather rigid and the cooperative and viscosity related relaxation increases rapidly with decreasing temperature. At such low temperatures, the water molecules are unable to perform motions on a longer length-scale due to confinement effects, and the dynamics follows an Arrhenius temperature dependence (Eq. 1.2). As the temperature is increasing, the strawberry matrix becomes more flexible and the water dynamics becomes more long-range. The activation energy of the water dynamics is reduced with increasing temperature, which gives that the water dynamics at higher temperatures is better described by a VFT temperature dependence (Eq. 1.3).

How the flexibility of the strawberry matrix is changed can furthermore be observed by the temperature induced changes of the ionic conductivity (Jansson *et al.* 2005). In the imaginary part of the dielectric permittivity, long-range ionic motions, that is, dc-conductivity, can generally be described by a power law ($(\sigma/(\varepsilon_0\omega)^n)$) behavior with an exponent n close to one. However, if the ions, which are giving rise to the conductivity, get stuck in cavities in the matrix (and the motion is restricted) so-called polarization effects occur and the exponent n displays a value lower than one. Thus, by following the temperature dependence of the exponent n it is possible to study structural changes by determine how the nature of the ionic motions changes with temperature. This is shown in Figure 1.5 for the hydrated strawberry. At low temperatures the value of the exponent is low (around 0.5), which indicates that the conductivity is mainly due to polarization effects. The matrix is rigid and the ionic motions are hindered to occur on a longer length-scale. As the temperature is increased the exponent n becomes larger and at around 250 K it shows a value close to one. Thus, with increasing temperature the matrix becomes more flexible and at 250 K the ions in the strawberry matrix no longer get stuck in confined geometries within the matrix, but instead are able to perform long-range migration.

1.3 Glass Transition and Relaxation Dynamics of Proteins

The glass transition of hydrated proteins has been shown to be exceptionally broad (Doster *et al.* 1986; Sartor *et al.* 1994; Miyazaki *et al.* 2000), and therefore, it can be difficult to observe, particularly at low hydration levels. The origin of the broadness has been discussed in the literature, and it has, for instance, been suggested that the hydration water forms clusters of different sizes on the protein surface (Doster *et al.* 1986), or that a large distribution of relaxation times is caused by a large number of relaxing local regions within the protein-water system (Sartor *et al.* 1994). Similar to the latter explanation we will here show that a number of different protein relaxations participate in the glass transition region of hydrated proteins (Jansson *et al.* 2010). We are able to make this conclusion by relating the calorimetric glass transition region ΔT_g, in the protein-solvent system, to the relaxation processes obtained by dielectric spectroscopy. To avoid ice formation at higher solvent contents and also to determine how the viscosity of the solvent affects the protein dynamics we have also studied the protein myoglobin

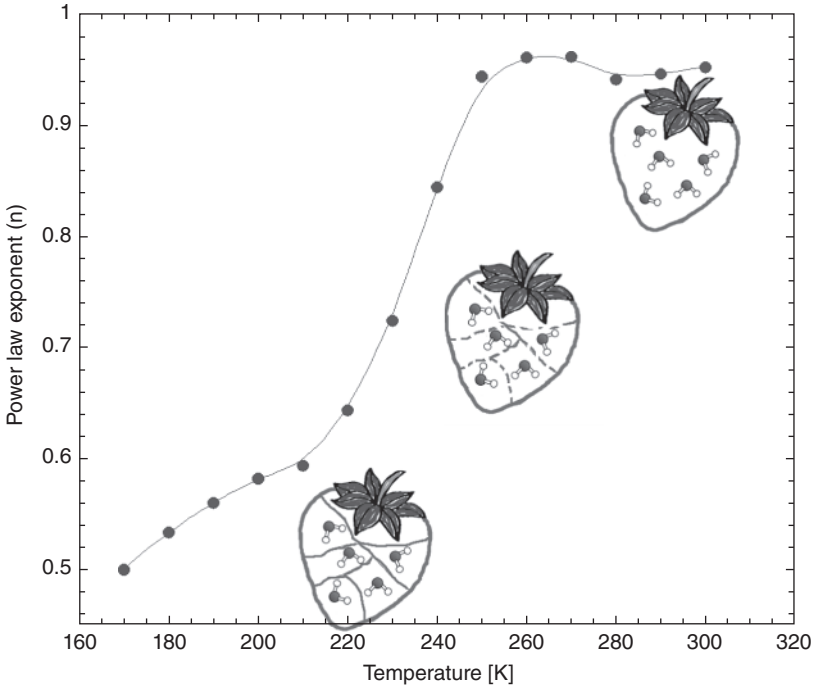

Figure 1.5 Temperature dependence of the power-law exponent *n* of the conductivity contribution ($(\sigma/(\varepsilon_0\omega)^n)$) to the imaginary part of the dielectric permittivity of the hydrated strawberry sample. The increase of *n* with increasing temperature is due to a transition from restricted ionic motions in cavities of the strawberry matrix to long-range ionic motions when the matrix is sufficiently mobile to "open up" the cavities. The figure is redrawn from Jansson *et al*. (Jansson *et al.* 2005).

in different mixtures of water and glycerol. In Figure 1.6e and f we present calorimetric results on myoglobin hydrated with h=0.5 and h=0.33 g water/g protein, respectively, and in A-D we show corresponding data for myoglobin in water-glycerol solvents of different amounts and concentrations (h is given by g solvent/g protein and wt% represents the weight fraction of water in the solvent). For all these samples a clear T_g can be observed. However, it should be noted that the step in heat flow (corresponding to a step in the heat capacity) is considerably weaker in the case of the two hydrated protein samples. It is particularly weak and broad for the low hydrated sample (h=0.33). Hence, the samples containing glycerol show a much stronger T_g, with a rapid change of the heat flow at the onset temperature and weaker "tail behaviour" close to its end point. The reason for this shape of the glass transition, and the difference compared to the hydrated protein samples, will be clear when the calorimetric and dielectric relaxation data are compared and discussed below.

From Figure 1.6, it is furthermore evident that the onset temperature of the glass transition is considerably less affected by the solvent composition than the end point of the transition, which shifts to higher temperatures with decreasing solvent content. This implies that also the width (taken from the onset to the end point temperature) of the transition increases with decreasing solvent content (Jansson *et al.* 2010; Jansson *et al.* 2011), as shown in Figure 1.7b. This figure further shows that the width of T_g

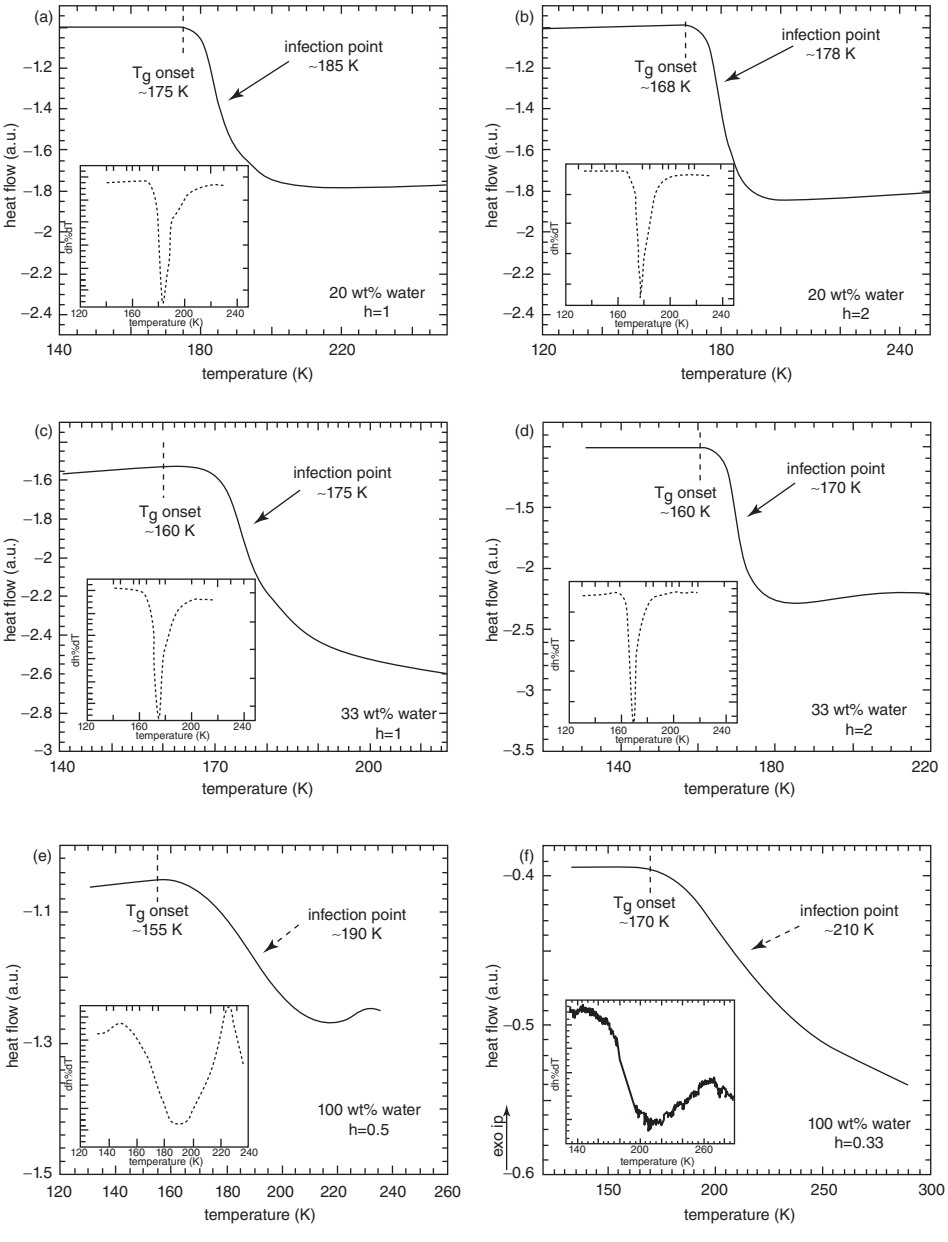

Figure 1.6 DSC curves obtained for myoglobin in water-glycerol mixtures. The water content in the solvent (in wt%) and the total solvent content h in g solvent per g myoglobin are given in each figure. The insets show the derivative of the heat flow with respect to the temperature, from which the broadness of the glass transition range was determined.

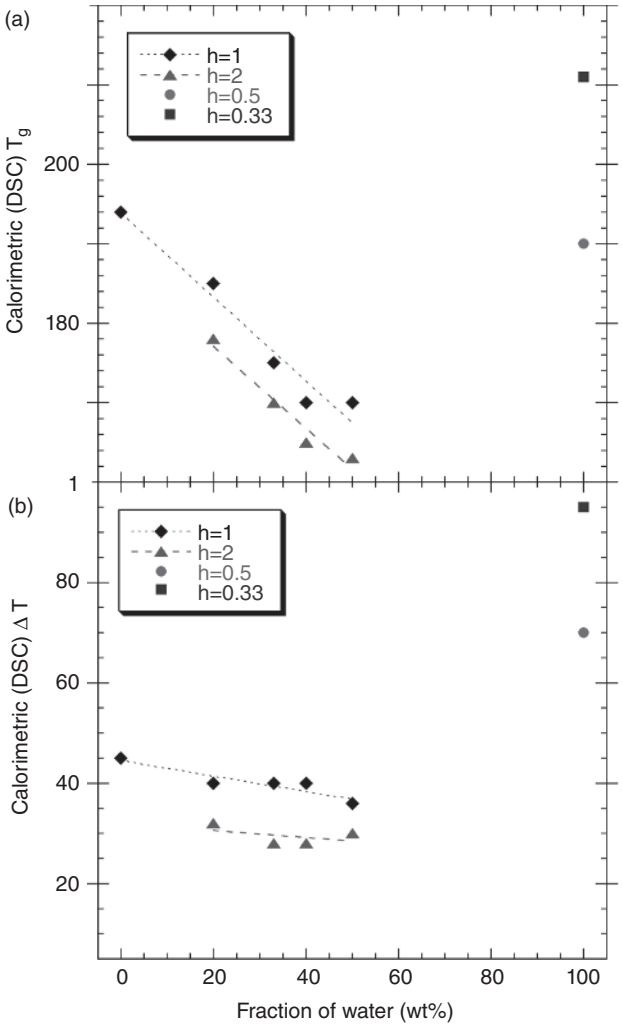

Figure 1.7 (a) Calorimetric glass transition temperature T_g (determined by the inflection point), and (b) broadness of the glass transition range ΔT_g (the whole transition range estimated from the derivative of the heat flow with respect to the temperature, as shown in the inset of Fig. 1.6)) are shown as a function of wt% water in the solvent for different solvent contents h. The error in ΔT_g is $\pm$5 K. The figure is redrawn from Jansson *et al*. (Jansson *et al.* 2011).

is much more dependent on the total solvent content than the total amount of water in the solvent, which suggests that not only the time scale of the solvent dynamics is important for the protein dynamics but also the amount of solvent, in agreement with findings from quasielastic neutron scattering (Jansson *et al.* 2009).

In Figure 1.8a, typical dielectric loss spectra are shown at different temperatures for the myogobin sample with a h=1 and 33 wt% water in the solvent (where a Teflon film was used to reduce contributions from dc conductivity and polarisation effects). The figure shows that several temperature dependent relaxation processes are present in the data. In order to extract the relaxation times of these processes, each process was fitted

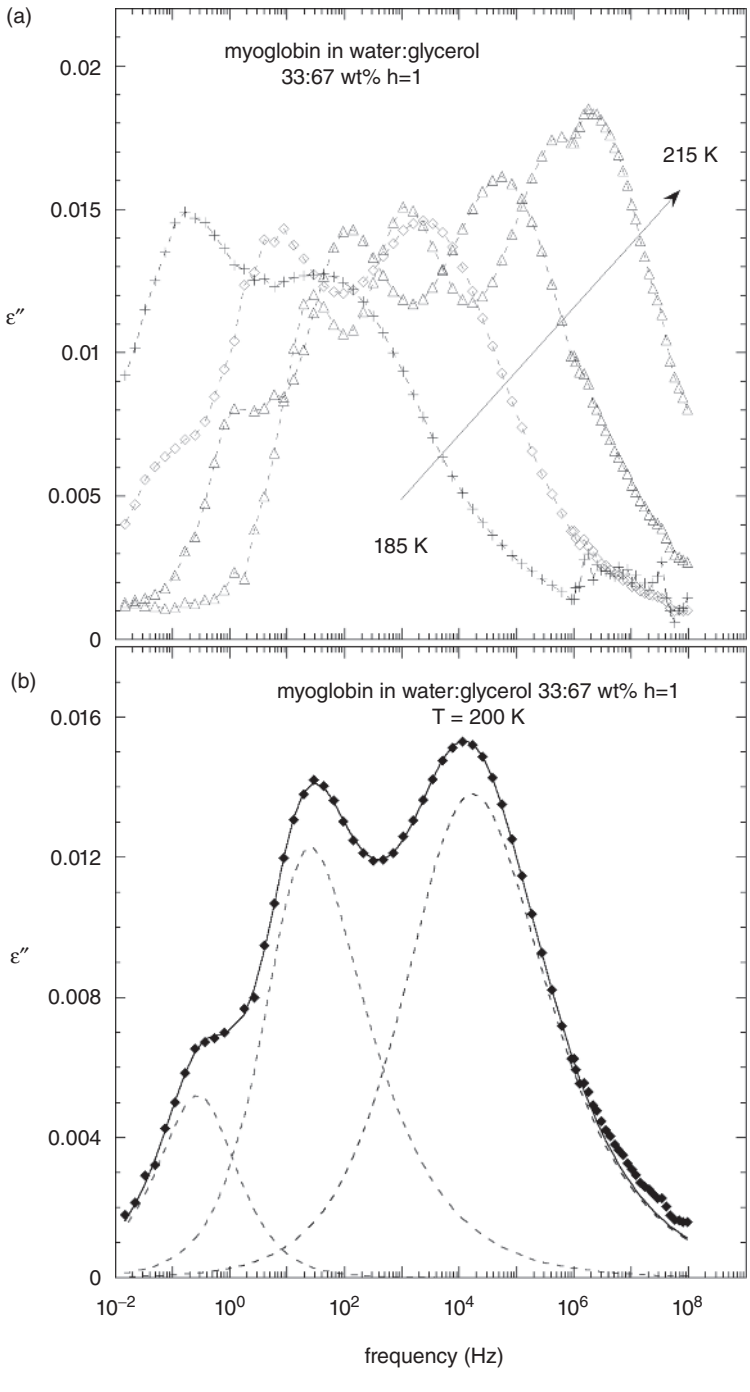

Figure 1.8 (a) Temperature evolution of the imaginary part of the dielectric permittivity vs frequency for myoglobin in a water-glycerol mixture of 33 wt% water and a total solvent content of h=1. In (b) the curve fitting is shown to visualize how the relaxation times of the different relaxation processes were extracted from the measured data. The figure is redrawn from Jansson *et al*. (Jansson, H. *et al.* 2011).

by the Havriliak-Negami function (Havriliak *et al.* 1967) (Eq. 1.4), except the slowest one for which a more general fit function (Bergman, 2000) (Eq. 1.5) was used.

$$\varepsilon''(\omega) = \sum \mathrm{IM}\left(\frac{\varepsilon_s - \varepsilon_\infty}{(1 + (\mathrm{i}\omega\tau)^\alpha)^\beta}\right) \tag{1.4}$$

$$\varepsilon''(\omega)\frac{\varepsilon_p''}{\frac{(1-C)}{a+b}[b(\omega/\omega_p)^{-a} + a(\omega/\omega_p)^b] + C} \tag{1.5}$$

In these equations $\omega = 2\pi f$ is the angular frequency. Specific parameters for the equations are in Eq. 1.4 the relaxation time τ, the static dielectric constant ε_s and the limiting value of the dielectric constant at high frequencies ε_∞. The shape parameters α and β determine the symmetric and asymmetric broadening of the relaxation peak, respectively. In Eq. 1.5 ω_p and ε_p'' are the position and the height of the peak. The parameters a and b are shape parameters that describe, in a log-log plot, the slope of the peak at low and high frequency side, respectively. C is a parameter that describes the broadening of the relaxation peak (without changing the power laws at high and low frequency sides). Figure 1.8b shows a typical fit to one of the spectra shown in Figure 1.8(a). At this temperature, three of totally four relaxation processes are clearly seen. The temperature dependences of the relaxation times extracted from the curve fitting procedure are shown in Figure 1.9 for the same samples as shown in Figure 1.6.

The VFT equation (Eq. 1.3) is used to describe global configurational changes of cooperative character, such as the α-relaxation, whereas Eq. 1.2 describes more local motions, such as β-relaxations. In Figure 1.9 we also show the calorimetric glass transition ranges, ΔT_g, obtained from the DSC data presented in Figure 1.6.

Let us now discuss the origin of the relaxation processes shown in Figure 1.9. The figure shows two solvent processes, where the fastest one (process I) is a local water process that is commonly observed in systems of confined supercooled water (Swenson *et al.* 2007). Most likely, this process is due to reorientations of single water molecules, but it will not be further discussed in this chapter since it does not seem to be related to any protein motions (Jansson *et al.* 2011). The second fastest process, denoted IIa or IIb depending on the temperature and sample composition, is due to the main relaxation of the solvent. This interpretation is unambiguous since it is very similar (only slightly slower) than the dielectric main relaxation of the corresponding bulk solvents (Hayashi *et al.* 2005; Puzenko *et al.* 2005). At low water contents (20 wt%), this process exhibits a non-Arrhenius temperature dependence over the whole temperature range. Even if this process (denoted IIa) mainly corresponds to the viscosity and glass transition related α-relaxation, there are results from quasielastic neutron scattering (QENQ) (Jansson *et al.* 2009) and time domain dielectric spectroscopy (TDDS) (Ermolina *et al.* 1994) that show that this process also contains a smaller contribution of local protein motions. At higher water contents it can be seen in Figure 1.9 that the α-relaxation (process IIa) in the solvent exhibits a dynamic crossover to a low temperature process (IIb) with an Arrhenius dependent relaxation time. The reason for this crossover is that a more local (β-like) w-relaxation decouples from the viscosity related α-relaxation in the solvent when it approaches its glass transition temperature. This low temperature process is mainly due to local motions of confined water molecules (Swenson *et al.* 2007; Vogel, 2008; Jansson *et al.* 2010; Lusceac *et al.* 2010) and most likely it has the same intermolecular origin as

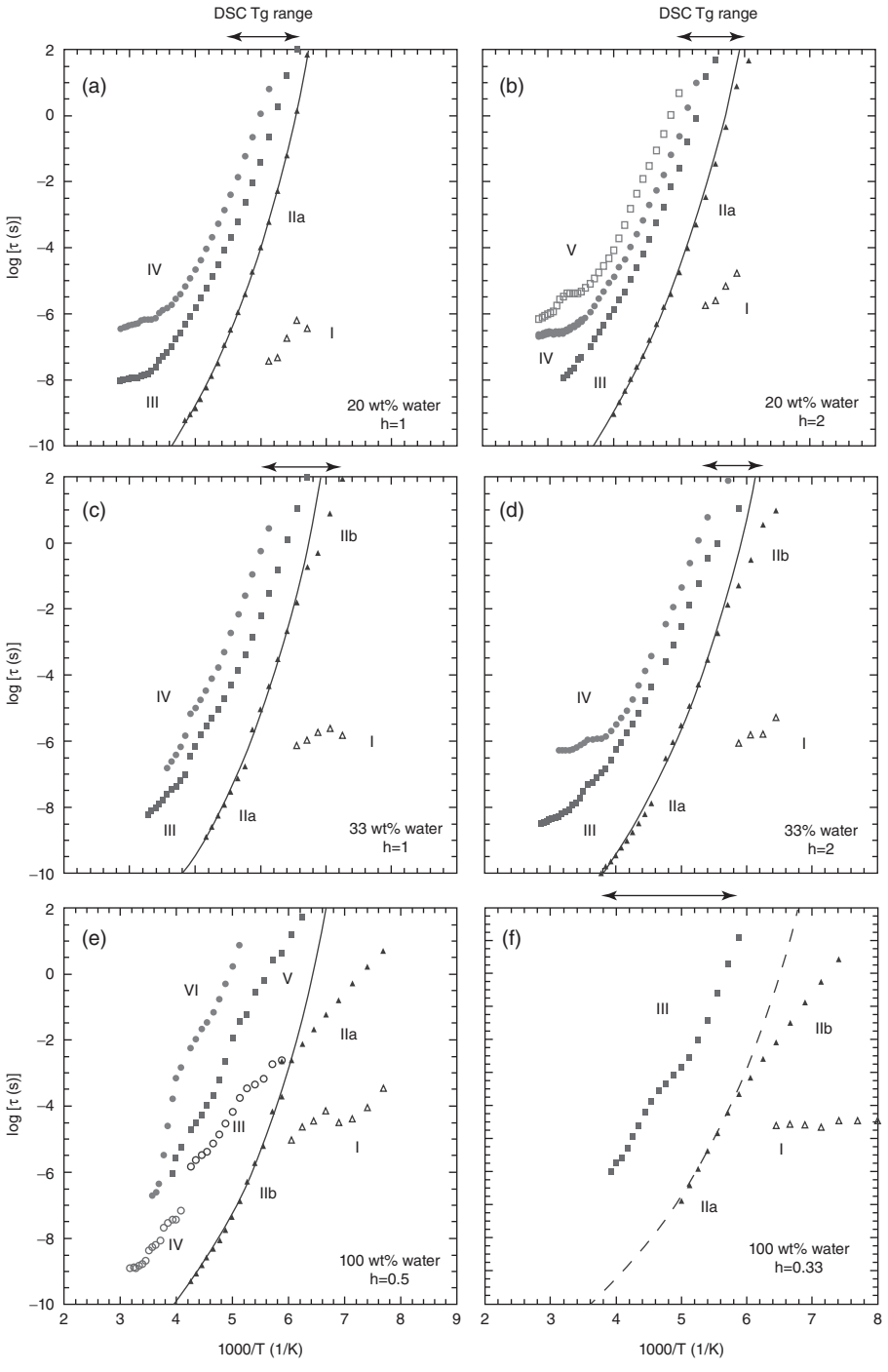

Figure 1.9 Dielectric relaxation times for the same six myoglobin samples as shown in Figure 1.6. Also shown in the figure are the calorimetric glass transition ranges, ΔT_g, obtained in Figure 1.6. The solid lines show the results of the curve fitting (by Eq. 1.3) of the temperature dependence of the main solvent relaxation in the high temperature range.

the Johari-Goldstein β-relaxation (Capaccioli *et al.* 2007). Below the crossover temperature the α-relaxation of the water-glycerol mixtures is generally weak compared to the local water relaxation and therefore it is difficult to observe (in case of hydration water it may not even exist (Swenson *et al.* 2006; Elamin *et al.* 2013)). Therefore, its temperature dependence is extrapolated by the VFT fits shown in Figure 1.9. If the time scale of the α-relaxation (process IIa) is compared for the different samples shown in Figure 1.9 it can be seen that this process becomes significantly faster with increasing water fraction for a given solvent content due to the plasticization effect of water. This process also becomes slightly faster with increasing total solvent content, since this leads to that a decreasing fraction of the solvent slows down by interactions with the protein. However, the water relaxation speeds up even more with increasing water fraction in the solvent, and therefore the decoupling (or crossover) becomes more pronounced for the water-rich samples.

From Figure 1.9 it is also evident that additional slower relaxation processes are present. For most of the samples two such slower processes are observed. The fastest one (process III) is attributed to arise from the relaxation of protein polar side groups, in agreement with earlier results from time-domain reflectometry (Bone, 1987). The time scale of this process is only slightly dependent on the composition of the solvent, which suggests that the composition of the solvent closest to the protein surface is more similar than the average composition. This interpretation is also supported by structural investigations, which have shown a preference of water at the protein surface (Sinibaldi *et al.* 2007). Similar findings are obtained for process IV (which is the slowest one except for myoglobin in the water-glycerol mixture of 20 wt% water and h=2), see Figure 1.9b. The exact origin of this process is not fully established, but both its relaxation time and temperature dependence is in excellent agreement with conformational changes of the protein structure as determined by hole-burning spectroscopy (Shibata *et al.* 1998).

For the two samples of hydrated myoglobin the low temperature water process (IIb in Figure 1.9e and f) reaches a relaxation time of 100 s at about 120 K. This temperature is far below the onset temperature of the broad T_g range, which from the DSC measurements is determined to occur from 160 K and 170 K, respectively (see Figure 1.6e and f). Since a local β-relaxation is not expected to participate in a glass transition, this observation further supports that the low temperature water relaxation cannot be a viscosity and glass transition related α-relaxation. Instead, the onset of the calorimetric T_g of these samples occurs at about the same temperature as the water relaxation exhibits the crossover to its low temperature Arrhenius dependence (see Figure 1.9e and f). This is also the temperature where the fastest observable protein relaxation (process III in Figure 1.9e and f) reaches a relaxation time of 100 s (i.e., on the time scale corresponding to a dynamical glass transition). This important finding strongly suggests that the onset of the calorimetric T_g occurs when the polar side groups of the protein start to move, that is, the time scale of the motions become faster than 100 s, and also that this onset of protein motions is caused by the crossover to more long-range diffusion (α-like fluctuations) in the surrounding water (Hedstrom *et al.* 2007; Jansson *et al.* 2011). Thus, the water is not giving any direct contribution to the calorimetric T_g, in agreement with the finding that water in hard confinements does not exhibits a clear calorimetric T_g (Elamin *et al.* 2013; Swenson *et al.* 2013) (see paragraph 4 below). Nevertheless, the hydration water is needed since no glass transition related protein motions can occur without large-scale motions in the solvent (Frauenfelder *et al.* 2009). Hence, in contrast

to most materials the glass transition is not an intrinsic property of proteins. Instead, the glass transition and other properties of proteins are driven by motions in the solvent, as further discussed below.

The absence of a direct contribution from water to the calorimetric T_g is in strong contrast to the behaviour for the protein samples in water-glycerol mixtures, where Figure 1.9 clearly shows that the α-relaxation in the solvent (process IIa) reaches a relaxation time of 100 s at about the same temperature as the onset of the calorimetric T_g. This finding is fully consistent with the observation that the corresponding bulk solvents exhibit a calorimetric T_g with a similar onset temperature. Thus, when the solvent contains glycerol the whole T_g range involves the freezing-in of both the α-relaxation in the solvent as well as different types of protein fluctuations. This difference between hydrated myoglobin and myoglobin in water-glycerol mixtures is evident from the DSC data shown in Figure 1.6. For the samples containing glycerol, the glass transition is asymmetric with an inflection point close to the onset of the T_g-range. In fact, these samples seem to contain at least two T_g components, one strong and narrow (as typical for ordinary liquids and solutions) at the lower part of the T_g-range and one weak and broad (as typical for hydrated proteins) at a slightly higher temperature, as seen in the insets of Figure 1.6. This is not the case for hydrated myoglobin, where only the weak and broad component can be observed (see Figure 1.6e and f). This implies that the freezing-in of the cooperative and viscosity related α-relaxation in the water-glycerol solvent makes a major contribution to the calorimetric T_g of these samples. This is in contrast to the glass transition of hydrated myoglobin where the main contribution, as discussed above, arises from protein motions occurring on different time scales (Jansson *et al.* 2010; Jansson *et al.* 2011). When these protein fluctuations occur on widely different time scales, the T_g-range becomes particularly broad in accordance with previous studies of the protein glass transition (Doster *et al.* 1986; Brownsey *et al.* 2003). Since all the dielectric processes shown in Figure 1.9 reach a time scale of 100 s at considerably lower temperatures than the end point of the calorimetric T_g-range this further implies that also other slower protein relaxations must contribute to the calorimetrically observed T_g, although these are obviously too weak to be observable in the dielectric measurements.

From the dielectric relaxation times shown in Figure 1.9 it is clear that these protein relaxation processes only occur above T_g, or above the dynamic crossover temperature in the case of hydrated myoglobin. Furthermore, it can be seen that the protein processes exhibit similar temperature dependences as the α-relaxation of the solvent. This is even more evident in Figure 1.10, where the relaxation times of the protein processes have been plotted as a function of the relaxation time for the α-process in the solvent (process IIa in Figure 1.9). The figure shows that there are linear dependences (i.e., slopes of unity in the log-log plots) for all the shown protein processes and sample compositions, although the dependences are less accurate for the hydrated samples (Figures 1.10e and f) where the protein processes are rather weak and it is difficult to extract the relaxation times with certainty (the error bars in the relaxation times are therefore somewhat larger than for samples of higher solvent content). Such identical temperature dependences for solvent and protein relaxations are, indeed, predicted by the "slaving model" (Frauenfelder *et al.* 1991; Fenimore *et al.* 2002; Frauenfelder *et al.* 2009). Therefore, our findings support the study by Fenimore *et al.* (Fenimore *et al.* 2002), where it was shown that the more global conformational changes of a protein are directly caused by the α-relaxation

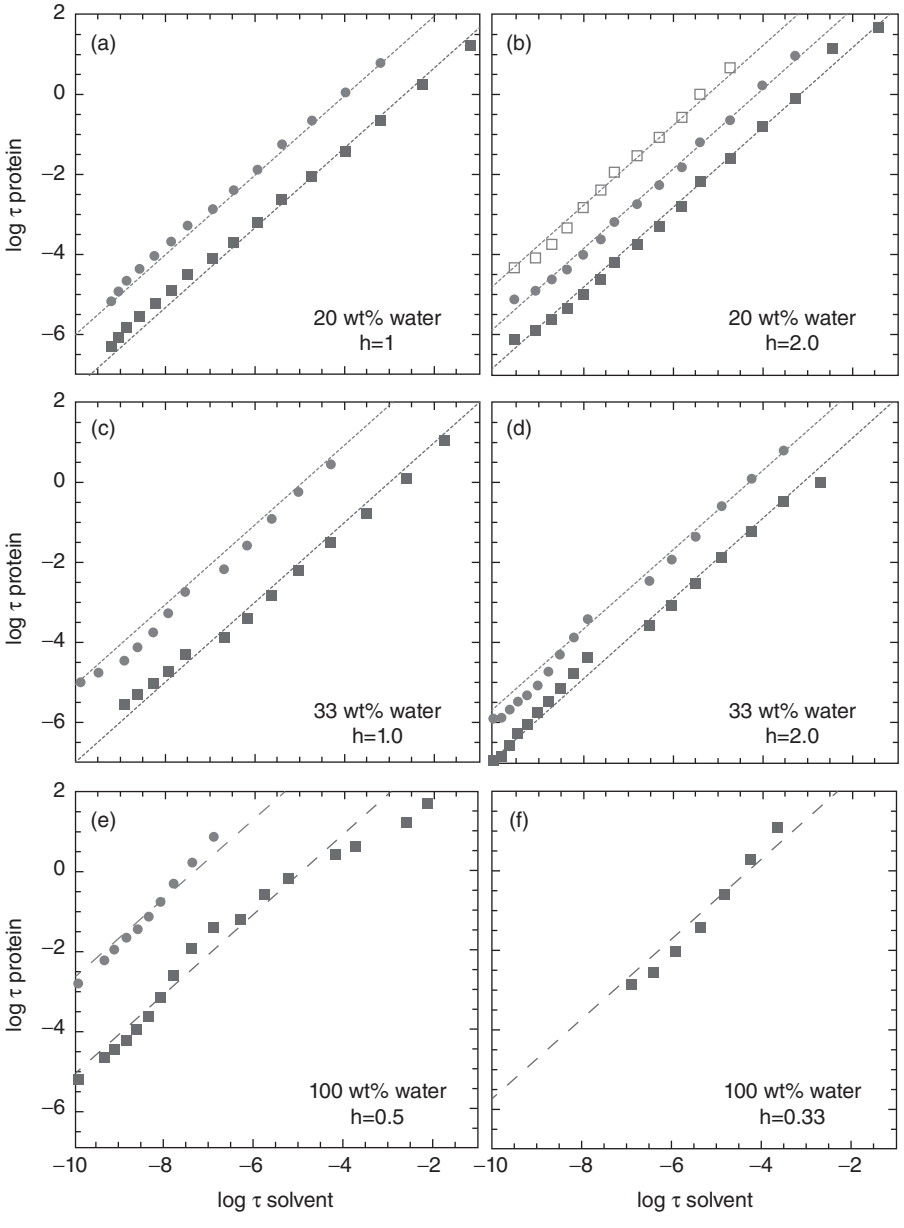

Figure 1.10 Relaxation times of the protein processes are shown as a function of the relaxation time of the α-process in the solvent. The protein processes are the same (same symbols) as shown in Figure 1.9. Note the almost perfect linear dependences for all protein processes and samples, except for the hydrated samples (e and f) where the temperature dependences of the protein relaxations are difficult to determine with good accuracy.

in the surrounding solvent. It should here be noted that the reason for that the protein motions are generally slower (typically 10^3 – 10^6 times slower) than the related α-relaxation in the solvent is that a conformational change of a protein often requires a large number of elementary steps, which can only take place if the solvent moves.

1.4 Confined Aqueous Solutions and the Failure of Gordon-Taylor Extrapolations to High-Water Contents

Let us now focus on what is happening with aqueous solutions of higher water contents, that is, in the dilute regime approaching pure water. As discussed in Section 1.2 above, such dilute solutions can unfortunately not be studied in the deeply supercooled regime without any substantial ice formation. The only way to reach such concentration and temperature ranges is to apply some kind of geometrical confinement to the solution. This "trick" was applied to glycerol (which normally do not crystallize), water and their mixtures by confining them in 21 Å pores of a MCM-41 silica matrix. The results obtained by DSC are shown in Figure 1.11 and, in agreement with previous studies of water confined in the same silica matrix (Takahara *et al.* 1999; Kittaka *et al.* 2006; Sjostrom *et al.* 2008; Yoshida *et al.* 2008), it is evident that no crystallization or melting events can be observed for any concentration, including pure water. In fact, 21 Å is the biggest pore size for which there is no obvious calorimetric signature of crystallization of water (Kittaka *et al.* 2006). Furthermore, it is directly evident from the figure that T_g is fairly constant in the concentration range up to 85 wt% water. This behaviour

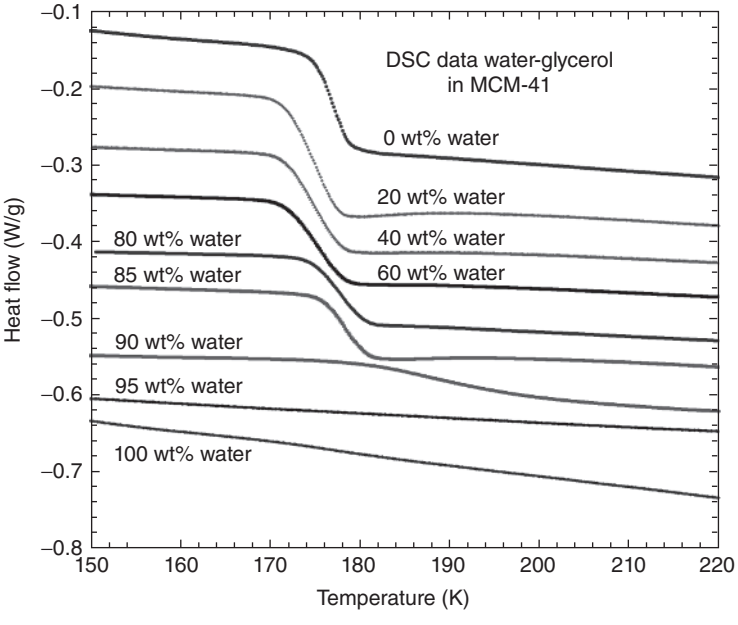

Figure 1.11 DSC heating scans of water-glycerol solutions confined in the 21 Å pores of MCM-41 C10. The concentration of water in each solution is given in the figure. The curves are vertically shifted for clarity. The figure is redrawn from Elamin *et al*. (Elamin *et al.* 2013).

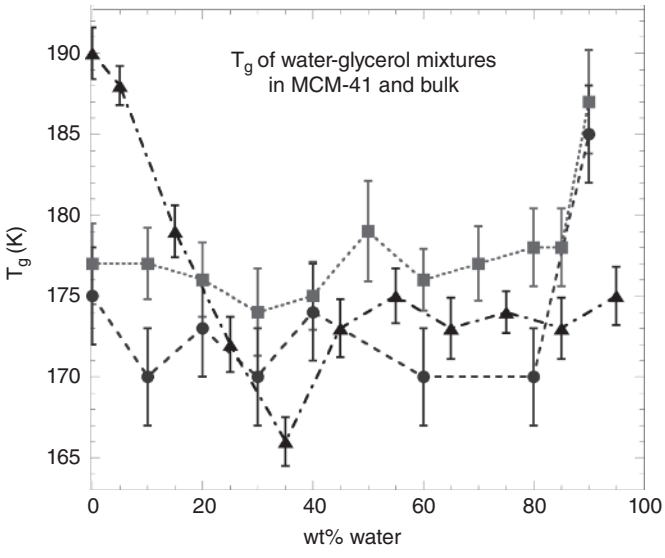

Figure 1.12 Concentration dependences of the glass transition temperature. Calorimetric values are shown for both confined solutions, obtained from the DSC data shown in Figure 1.11 (solid squares), and bulk solutions (open squares). Dynamic glass transitions, estimated as the temperature where the α-relaxation reaches a time scale of 100 s, are also shown for the confined solutions (solid circles). The dashed lines between the data points are just a guide for the eye. The figure is redrawn from Elamin *et al*. (Elamin *et al.* 2013).

is in strong contrast to the concentration dependence of T_g for the corresponding bulk solutions, where a pronounced plasticization effect of water is evident up to a water concentration of about 40 wt% (where crystallization occurs), as seen in Figure 1.12. (At higher water concentrations the bulk solutions become freeze-concentrated with an effective water concentration of about 22 wt%). The almost concentration independent T_g of the confined solutions up to 85 wt% water can be explained by a surface-induced micro-phase separation of the mixtures into two more or less separate liquids. The reason for this micro-phase separation should be that water has a stronger tendency to coordinate to the hydroxyl groups of the inner pore surface, leaving most of the glycerol molecules clustered in the centre of the pores. The observed T_g should then be associated with the glass transition of the glycerol clusters, since the confined water molecules do not give rise to any T_g feature, as seen in Figure 1.11 and as further discussed below. The almost concentration independent T_g is then expected to remain until the glycerol part becomes so diluted that no significant glycerol clusters are formed. This is likely what is seen in Figure 1.11 at 90 wt% water, where the very broad step of T_g suggests that the glycerol molecules have widely different local environments. From Figures 1.11 and 1.12 it is also evident that T_g increases rapidly at very high water concentrations of around 90 wt%. However, let us wait to discuss the implications of this observation and first focus on the rapid decrease of the amplitude of the calorimetric glass transition with increasing water content at the highest water concentrations. The observation in Figure 1.11, that no T_g can be detected for the present sample of confined water, is in agreement with previous studies of supercooled water confined in different types of host materials (Takahara *et al.* 1999; Swenson 2004; Kittaka *et al.* 2006; Swenson *et al.* 2006;

Hedstrom *et al.* 2007; Swenson *et al.* 2007; Johari, 2009; Kittaka *et al.* 2009; Jansson *et al.* 2010; Jansson *et al.* 2011; Swenson *et al.* 2013). Thus, the present findings are very similar to what we observed for proteins in Section 1.3, where a water-glycerol solvent gave a major contribution to the calorimetric T_g in contrast to a hydrated protein, where the hydration water gave no direct contribution to the broad T_g of the protein (Jansson *et al.* 2010; Jansson *et al.* 2011).

The observation that no clear calorimetric T_g can be observed for confined water is puzzling since most types of liquids, of which glycerol is one example, exhibit a calorimetric glass transition and an associated structural relaxation process provided that the confinement is not extremely severe in comparison to the size of the molecules (Swenson *et al.* 2006). A possible explanation for the unique behaviour of confined water might be that there is a reduced possibility for the water molecules in the confinement to access the same configurational space as in bulk water, that is, a smaller number of structural configurations may be accessible in the confinement, which, in turn, should reduce the step in the heat capacity, ΔC_p, at T_g. Since even the most accepted T_g of bulk water at 136 K is associated with only a small ΔC_p of about 2 J mol^{-1} K^{-1} (Hallbrucker *et al.* 1989) it is possible that T_g of confined water becomes so weak that it cannot be observed in an ordinary DSC measurement. Another hypothesis for why no calorimetric T_g can be detected for confined water is that the molecular rearrangements responsible for the glass transition of bulk water require an extended three-dimensional network of hydrogen bonded water molecules, which simply cannot be formed in pore sizes of about 20 Å or less. This hypothesis is further supported by the belief that a hydrogen bonded tetrahedral network structure is completed in bulk water around the homogenous nucleation temperature of about 235 K (Ito *et al.* 1999). Such a network structure may lead to viscosity-related molecular rearrangements of exceptionally large volumes. Furthermore, the rapid growing of these cooperatively rearranging regions in this temperature range may cause a similar rapid increase of the glass transition related structural relaxation time, leading to a true T_g of bulk water as high as 228 K (Swenson *et al.* 2010), where dynamical quantities, such as viscosity and diffusion constant, seem to extrapolate to infinity (Speedy *et al.* 1976; Hodge *et al.* 1978). The present findings for the confined water-glycerol solutions support this latter hypothesis, as further discussed below.

The results from the DSC measurements, presented in Figures 1.11 and 1.12, showing that T_g is almost concentration independent up to 85 wt% water and thereafter increases rapidly at the highest water contents, at the same time as its calorimetric feature decreases to an infinitely small signal for confined water, are supported by dielectric relaxation measurements. Figure 1.13 shows how the time scale of the viscosity related structural α-relaxation is fairly concentration independent up to 80 wt% water, but that it increases substantially at 90 wt% water, and thereafter vanish (at least at low temperatures) for the sample of confined water. Thus, both the calorimetric and dielectric relaxation data provide the same picture of a slowing down of the viscosity related dynamics when the concentration approaching confined water, but that this dynamics also vanish before that concentration is reached. This implies that only a more local water (w-) relaxation, which is similar to the β-relaxation of confined glycerol, can be observed for confined water at low temperatures, see Figure 1.13. This local relaxation process is similar for all concentrations. However, only the sample of confined water is lacking the slower α-relaxation, with its characteristic non-Arrhenius temperature dependence and

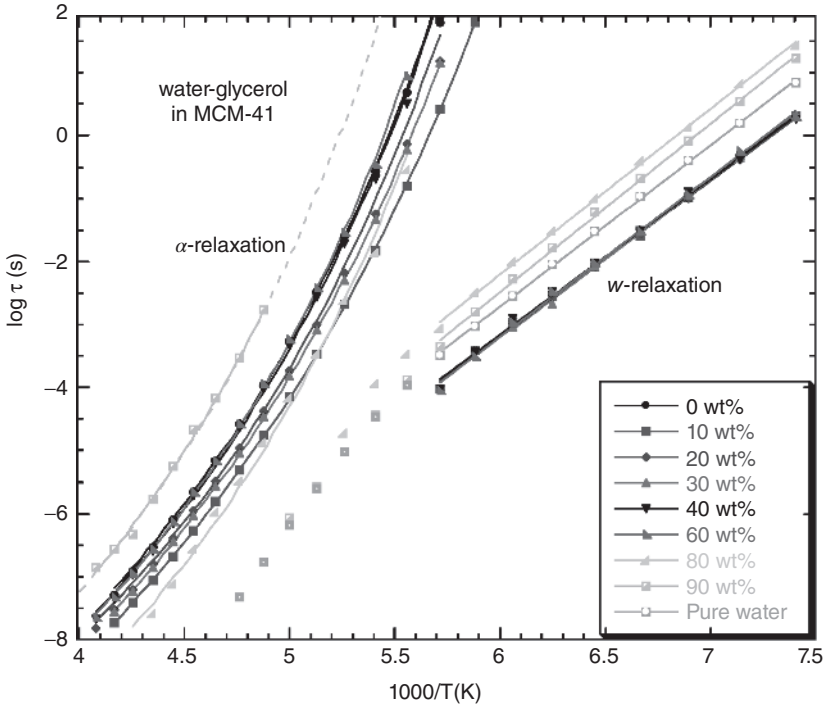

Figure 1.13 Arrhenius plot of dielectric relaxation times of the α and w (or β) processes of the confined solutions. The water concentration of each sample is given in the figure. The figure is redrawn from Elamin *et al*. (Elamin *et al.* 2013).

its strong relation to the calorimetric T_g. The latter implies that a dynamical glass transition temperature can be estimated as the temperature for which the α-relaxation reaches a time scale of 100 s. Such T_g values have been estimated from Figure 1.13, and are presented in Figure 1.12 in comparison with the calorimetric T_g. The slightly lower values of the dynamic T_g can be explained by the fact the calorimetric T_g-values were defined as the inflection point in the step of the heat capacity, instead of its onset temperature, which commonly gives a better agreement with dielectric estimations of T_g.

Let us now return to the observation of a rapidly increased T_g at the highest water concentrations. In Figure 1.12 it can be seen that the "average T_g-value" for water concentrations up to 80 wt% increases from around 176 K to about 187 K at 90 wt% water (for the dielectrically determined dynamic T_g the increase is even larger). This implies that the surrounding water molecules have an antiplasticization effect on the glycerol molecules in this concentration and temperature range. However, due to the large amount of water and the low solute concentration it is more appropriate to express it the other way around, that is, that glycerol has a plasticization effect on the confined water. Considering the knowledge we have about deeply supercooled water this is not a surprising finding since the glycerol molecules are expected to break up, and thereby softens, the nearly tetrahedral network structure of the confined water in the temperature range of T_g. Thus, the addition of solute molecules to deeply supercooled confined water is likely to reduce the hydrogen bonding, leading to an increased flexibility and

more mobile molecules than in the more rigid tetrahedral network structure of pure water at these temperatures. In fact, this plasticization effect of solute molecules on the glass transition related dynamics of deeply supercooled water should have a similar origin as the commonly observed confinement induced speeding up of the same dynamics close to T_g (Alcoutlabi *et al.* 2005). Both the addition of "guest molecules", such as glycerol, and geometrical confinements reduce the average number of hydrogen bonds in supercooled water (Rovere *et al.* 1998), and thereby increase the flexibility of the network structure and, consequently, the water molecules become more mobile. This further implies that, in our case when the water is affected by both guest molecules (i.e., glycerol) and a confining geometry, the observed T_g of about 187 K at 90 wt% water should be considerably lower than for bulk water, where a value above 200 K is expected from the present study. In agreement with these findings and interpretations is also a fast scanning calorimetry study of diluted aqueous bulk solutions, showing that guest molecules have a similar plasticization effect also on bulk water (McCartney *et al.* 2013). Also this study supported a T_g of bulk water above 200 K (McCartney *et al.* 2013).

From several previous studies (Elamin *et al.* 2013; McCartney *et al.* 2013) as well as the present study it is evident that the Gordon-Taylor equation cannot be used to estimate T_g of pure water or highly diluted aqueous solutions from the more concentrated aqueous solutions, since the monotonic concentration dependence the Gordon-Taylor equation is based on is not maintained at the highest water concentrations. Thus, since most aqueous solutions crystallize at water concentrations above approximately 40 wt% the extrapolations have to be based on the concentration dependence observed in the range where water generally has a plasticization effect on the other component, as shown in Figure 1.12 for the water-glycerol bulk solutions up to 35 wt% water where no ice is formed during cooling. This implies that the completely different behaviour we observe at very high water concentrations is not considered in such extrapolations. This also means that the use of the Gordon-Taylor equation (Gordon *et al.* 1952), to support a T_g of bulk water around 135 K, is incorrect, despite its common approach in the literature.

1.5 Concluding Discussion

In this chapter the glass transition and its related dynamics of water containing materials have been discussed. It has been shown that the properties of these materials are strongly determined by their water contents. In the case of food materials and sugar solutions the water is mainly giving rise to a strong plasticizing effect on the system, which reduces its glass transition temperature dramatically. However, as shown for the confined solutions in Section 1.4, this plasticizing effect of water does not continue to very high water contents, due to the strong network character of the hydrogen bonds in deeply supercooled water. Thus, water behaves very differently in systems of low and high water contents, and this, in turn, leads to a breakdown of the Gordon-Taylor equation (Gordon *et al.* 1952) at high water contents.

In the case of proteins, the surrounding water plays an even more important role since proteins would be un-functioning without an appropriate solvent. The water is directly causing the protein motions that are required for their biological activities (Frauenfelder *et al.* 1991; Vitkup *et al.* 2000; Tarek *et al.* 2002; Fenimore *et al.* 2004; Doster *et al.* 2005).

Thus, the protein functions are "slaved" by the motions in the surrounding water. However, the glass transition range of hydrated myoglobin, as also shown in Figure 1.9e and f, is located at a too high temperature and is too broad to be associated with a glass transition of the hydration water. An extrapolation of process IIa to a relaxation time of 100 s gives a dynamic glass transition temperature of about 150 K, which is far below the temperature range of the observed glass transition. Hence, even if the α-relaxation of the hydration water (process IIa) had continued below the crossover temperature at 160–170 K it had not been possible to associate it with the observed calorimetric glass transition. However, the lack of an observable calorimetric glass transition of the protein hydration water is fully consistent with calorimetric and dielectric results on water confined in other types of systems (Swenson *et al.* 2007; Sjostrom *et al.* 2008; Cerveny *et al.* 2010). Thus, protein hydration water is no exception, but behaves both calorimetrically and dielectrically as interfacial water in general. The reason for that interfacial water lack a clear calorimetric glass transition is not fully clear, but most likely motions associated to the glass transition (i.e., the viscosity related α-relaxation) vanish before the glass transition temperature is reached, as also suggested from the dielectric relaxation measurements where no α-relaxation can be observed for the hydration water below the dynamic crossover temperature. This relaxation behaviour of confined water can be understood from Figure 1.14, which shows schematic scenarios of the temperature dependent dynamics of a typical bulk liquid (A) and confined water (B). The typical non-Arrhenius temperature dependence of the viscosity related α-relaxation in a bulk liquid (A) is commonly explained by an increasing number of molecules (i.e., an increasing length-scale) involved in the cooperative rearrangement of molecules associated to the relaxation process. However, if the length-scale of this cooperativity exceeds the size of a geometrical confinement (B) the cooperativity length can no longer grow with

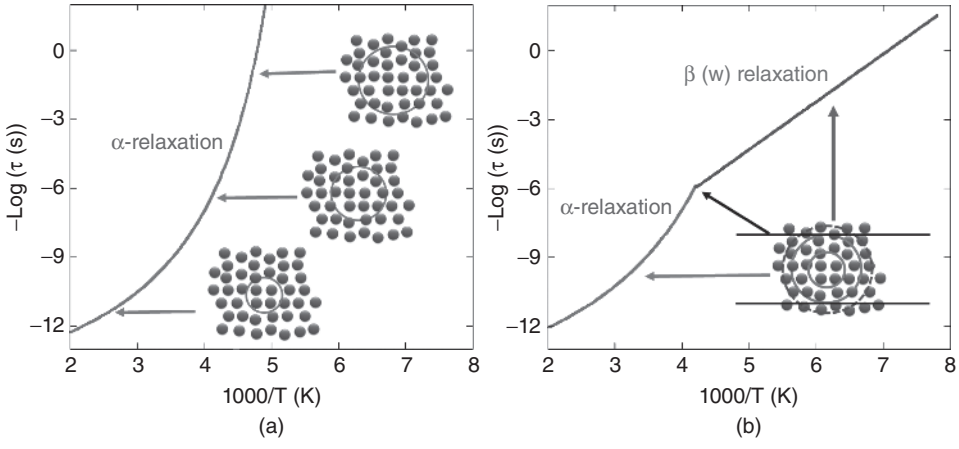

Figure 1.14 (a) A schematic description of a typical temperature dependence of the viscosity related α-relaxation in a bulk liquid. The figure shows how the activation energy increases with decreasing temperature due to an increasing number of molecules involved in the cooperative rearrangement of molecules associated to the relaxation process. (b) A possible relaxation scenario for confined water. In this case the length-scale of the cooperativity can no longer grow with decreasing temperature if the cooperativity length exceeds the size of the geometrical confinement. Instead, a crossover to a more local (β-like) relaxation occurs. Figure (a) is redrawn from Monasterio *et al.* (Monasterio *et al.* 2013).

decreasing temperature, and this may prevent this type of viscosity related relaxation process to occur. Instead, a crossover to a more local (β-relaxation) occurs, since this process should not be substantially affected by the restricted geometry.

To conclude, in this chapter we have discussed how water behaves in biological and food related materials and how the presence of this water affects the dynamical properties of these materials. The results indicate that water not only exhibits, and gives rise to, some universal features, but also that the relaxation properties of these water containing systems are fairly poorly understood, particularly in the deeply supercooled regime close to T_g. The important hydrogen bonding of water can also influence the structural and dynamical properties of a system very differently depending on the chemical natures of the other components in the system. Therefore, plasticization effects as well as antiplasticization effects of water can be obtained, and these effects may shift with the water content. This makes it impossible to predict the concentration dependence of the dynamics and T_g over wide water concentration ranges. To understand the dynamical behaviour of supercooled water and its implications for the properties of water containing systems it is clear that further investigations of the role of water and its hydrogen bonds for material properties are needed.

References

Alcoutlabi, M. and McKenna, G.B. (2005) Effects of confinement on material behaviour at the nanometre size scale. *Journal of Physics-Condensed Matter*, 17: R461–R524.

Angell, C.A. (1991) Relaxation in liquids, polymers and plastic crystals – strong fragile patterns and problems. *Journal of Non-Crystalline Solids*, 131: 13–31.

Angell, C.A. (2008) Insights into phases of liquid water from study of its unusual glass-forming properties. *Science*, 319: 582–587.

Antognozzi, M., Humphris, A.D.L., and Miles, M.J. (2001) Observation of molecular layering in a confined water film and study of the layers viscoelastic properties. *Applied Physics Letters*, 78: 300–302.

Bergman, R. (2000) General susceptibility functions for relaxations in disordered systems. *Journal of Applied Physics*, 88: 1356–1365.

Bone, S. (1987) Time-domain reflectometry studies of water binding and structural flexibility in chymotrypsin. *Biochimica Et Biophysica Acta*, 916: 128–134.

Brownsey, G.J., Noel, T.R., Parker, R., and Ring, S.G. (2003) The glass transition behavior of the globular protein bovine serum albumin. *Biophysical Journal*, 85: 3943–3950.

Capaccioli, S., Ngai, K.L., and Shinyashiki, N. (2007) The Johari-Goldstein beta-relaxation of water. *Journal of Physical Chemistry B*, 111: 8197–8209.

Cerveny, S., F., B.-B., Alegriá, A., and Colmenero, J. (2010) Dynamics of water intercaleted in graphite oxide. *Journal of Physical Chemistry*, 114: 2604–2612.

Chen, S.H., Liu, L., Fratini, E., Faraone, A., and Mamontov, E. (2006) Observation of fragile-to-strong dynamic crossover in protein hydration water. *Proceedings of the National Academy of Sciences of the United States of America*, 103: 9012–9016.

Doster, W., Bachleitner, A., Dunau, R., Hiebl, M., and Luscher, E. (1986) Thermal properties of water in myoglobin crystals and solutions at subzero temperatures. *Biophysical Journal*, 50: 213–219.

Doster, W. and Settles, M. (2005) Protein-water displacement distributions. *Biochimica Et Biophysica Acta-Proteins and Proteomics*, 1749: 173–186.

Elamin, K., Jansson, H., Kittaka, S., & Swenson, J. (2013) Different behavior of water in confined solutions of high and low solute concentrations. *Physical Chemistry Chemical Physics*, 15: 18437–18444.

Ermolina, I., Fedotov, V., Feldman, Y., and Ivoylov, I. (1994) Investigation of Molecular-Motion and Interprotein Interactions in Solutions by TDDS – a Comparison with NNM Data. *Journal of Non-Crystalline Solids*, 172: 1103–1108.

Faraone, A., Liu, L., Mou, C.Y., Yen, C.W., and Chen, S.H. (2004) Fragile-to-strong liquid transition in deeply supercooled confined water. *Journal of Chemical Physics*, 121: 10843–10846.

Fenimore, P.W., Frauenfelder, H., McMahon, B.H., and Parak, F.G. (2002) Slaving: Solvent fluctuations dominate protein dynamics and functions. *Proceedings of the National Academy of Sciences of the United States of America*, 99: 16047–16051.

Fenimore, P.W., Frauenfelder, H., McMahon, B.H., and Young, R.D. (2004) Bulk-solvent and hydration-shell fluctuations, similar to alpha- and beta-fluctuations in glasses, control protein motions and functions. *Proceedings of the National Academy of Sciences of the United States of America*, 101: 14408–14413.

Franks, F. and Mathias, S. (eds) (1983). *Biophysics of Water*. Wiley, London.

Frauenfelder, H., Chen, G., Berendzen, J., Fenimore, P.W., Jansson, H., McMahon, B.H., Mihut-Stroe, I., Swenson, J., and Young, R.D. (2009) A unified model of protein dynamics. *Proceedings of the National Academy of Sciences*, 106: 5129–5134.

Frauenfelder, H. and Gratton, E. (1986) Protein dynamics and hydration. *Methods in Enzymology*, 127: 207–216.

Frauenfelder, H., Sligar, S.G., and Wolynes, P.G. (1991) The energy landscapes and motions of proteins. *Science*, 254: 1598–1603.

Fulcher, G.S. (1925) Analysis of recent measurements of the viscosity of glasses. *Journal of the American Ceramic Society*, 8: 339–355.

Gallat, F.-X., Brogan, A.P.S., Fichou, Y., McGrath, N., Moulin, M., Haertlein, M., Combet, J., Wuttke, J., Mann, S., Zaccai, G., Jackson, C.J., Perriman, A.W., and Weik, M. (2012) A polymer surfactant corona dynamically replaces water in solvent-free protein liquids and ensures macromolecular flexibility and activity. *Journal of the American Chemical Society*, 134: 13168–13171.

Goldstein, D.L., Frisbie, J., Diller, A., Pandey, R.N., and Krane, C. M. (2010) Glycerol uptake by erythrocytes from warm- and cold-acclimated Cope's gray treefrogs. *Journal of Comparative Physiology B-Biochemical Systemic and Environmental Physiology*, 180: 1257–1265.

Gordon, M. and Taylor, J.S. (1952) Ideal copolymers and the 2nd order transitions of synthetic rubbers 1. Non-crystalline copolymers. *Journal of Applied Chemistry*, 2: 493–500.

Gunning, Y.M., Gunning, P.A., Kemsley, E.K., Parker, R., Ring, S.G., Wilson, R.H., and Blake, A. (1999) Factors affecting the release of flavor encapsulated in carbohydrate matrixes. *Journal of Agricultural and Food Chemistry*, 47: 5198–5205.

Hallbrucker, A., Mayer, E., and Johari, G.P. (1989) Glass-liquid transition and the enthalpy of devitrification of annealed vapor- deposited amorphous solid water – a comparision with hyperquenched glass water. *Journal of Physical Chemistry*, 93: 4986–4990.

Havriliak, S. and Negami, S. (1967) A complex plane representation of dielectric and mechanical relaxation processes in some polymers. *Polymer*, 8: 161–210.

Hayashi, Y., Puzenko, A., Balin, I., Ryabov, Y.E., and Feldman, Y. (2005) Relaxation dynamics in glycerol-water mixtures. 2. Mesoscopic feature in water rich mixtures. *Journal of Physical Chemistry B*, 109: 9174–9177.

Hedstrom, J., Swenson, J., Bergman, R., Jansson, H., Kittaka, S. (2007) Does confined water exhibit a fragile-to-strong transition? *European Physical Journal-Special Topics*, 141: 53–56.

Hodge, I.M. and Angell, C.A. (1978) Relative permittivity of supercooled water *Journal of Chemical Physics*, 68: 1363–1368.

Ito, K., Moynihan, C.T. and Angell, C.A. (1999) Thermodynamic determination of fragility in liquids and a fragile-to-strong liquid transition in water. *Nature*, 398: 492–495.

Jansson, H., Bergman, R., and Swenson, J. (2005) Dynamics of sugar solutions as studied by dielectric spectroscopy. *Journal of Non-Crystalline Solids*, 351: 2858–2863.

Jansson, H., Bergman, R., and Swenson, J. (2011) Role of solvent for the dynamics and the glass transition of proteins. *Journal of Physical Chemistry B*, 115: 4099–4109.

Jansson, H., Huldt, C., Bergman, R., and Swenson, J. (2005) Dynamics of water in strawberry and red onion as studied by dielectric spectroscopy. *Physical Review E*, 71: 011901.

Jansson, H., Kargl, F., Fernandez-Alonso, F., and Swenson, J. (2009) Dynamics of a protein and its surrounding environment; A QENS study of myoglobin in water and glycerol mixtures. *Journal of Chemical Physics*, 130: 205101–205113.

Jansson, H. and Swenson, J. (2003) Dynamics of water in molecular sieves by dielectric spectroscopy. *European Physical Journal E*, 12: S51–S54.

Jansson, H. and Swenson, J. (2010) The protein glass transition as measured by dielectric spectroscopy and differential scanning calorimetry. *Biochimica et Biophysica Acta: Proteins and Proteomics*, 1804: 20–26.

Jensen, M.O., Mouritsen, O.G., Peters, G.H. (2004) The hydrophobic effect: Molecular dynamics simulations of water confined between extended hydrophobic and hydrophilic surfaces. *Journal of Chemical Physics*, 120: 9729–9744.

Johari, G.P. (2009) Origin of the enthalpy features of water in 1.8 nm pores of MCM-41 and the large Cp increase at 210 K. *Journal of Chemical Physics*, 130: 124518.

Johari, G.P., Hallbrucker, A., & Mayer, E. (1987) The glass liquid transition of hyperquenched water. *Nature*, 330: 552–553.

Kittaka, S., Ishimaru, S., Kuranishi, M., Matsuda, T., and Yamaguchi, T. (2006) Enthalpy and interfacial free energy changes of water capillary condensed in mesoporous silica, MCM-41 and SBA-15. *Physical Chemistry Chemical Physics*, 8: 3223–3231.

Kittaka, S., Sou, K., Yamaguchi, T., and Tozaki, K.-i. (2009) Thermodynamic and FTIR studies of supercooled water confined to exterior and interior of mesoporous MCM-41. *Physical Chemistry Chemical Physics*, 11: 8538–8543.

Levine, H. and Slade, L. (1990). *Thermal Analysis of Foods*. Elsevier Applied Science Publishers, London.

Liu, L., Chen, S.H., Faraone, A., Yen, C.W. and Mou, C.Y. (2005) Pressure dependence of fragile-to-strong transition and a possible second critical point in supercooled confined water. *Physical Review Letters*, 95: 117802.

Luby-Phelps, K., Lanni, F., and Taylor, D.L. (1988) The submicroscopic properties of cytoplasm as a determinant of cellular function. *Annual Review of Biophysics and Biophysical Chemistry*, 17: 369–396.

Lusceac, S.A. and Vogel, M. (2010) ^{2}H NMR Study of the Water Dynamics in Hydrated Myoglobin. *Journal of Physical Chemistry B*, 114: 10209–10216.

Mallamace, F., Broccio, M., Corsaro, C., Faraone, A., Wanderlingh, U., Liu, L., Mou, C.Y., and Chen, S.H. (2006) The fragile-to-strong dynamic crossover transition in confined water: nuclear magnetic resonance results. *Journal of Chemical Physics*, 124: 161102.

Mathews, C.K., van Holde, K.E., and Ahern K.G. (eds) (2000). *Biochemistry 3rd edition*. San Fransisco, Addison Wesley Longman.

McCartney, S.A. and Sadtchenko, V. (2013) Fast scanning calorimetry studies of the glass transition in doped amorphous solid water: Evidence for the existence of a unique vicinal phase. *Journal of Chemical Physics*, 138: 084501.

Miyazaki, Y., Matsuo, T., and Suga, H. (2000) Low-temperature heat capacity and glassy behavior of lysozyme crystal. *Journal of Physical Chemistry B*, 104: 8044–8052.

Monasterio, M., Jansson, H., Gaitero, J.J., Dolado, J.S., and Cerveny, S. (2013) Cause of the fragile-to-strong transition observed in water confined in C-S-H gel. *Journal of Chemical Physics*, 139: 164714

Puzenko, A., Hayashi, Y., Ryabov, Y.E., Balin, I., Feldman, Y., Kaatze, U., and Behrends, R. (2005) Relaxation dynamics in glycerol-water mixtures: I. Glycerol-rich mixtures. *Journal of Physical Chemistry B*, 109: 6031–6035.

Rariy, R.V. and Klibanov, A.M. (1997) Correct protein folding in glycerol. *Proceedings of the National Academy of Sciences of the United States of America*, 94: 13520–13523.

Raviv, U., Laurat, P., and Klein, J. (2001) Fluidity of water confined to subnanometre films. *Nature*, 413: 51–54.

Rexer-Huber, K.M.J., Bishop, P.J., and Wharton, D.A. (2011) Skin ice nucleators and glycerol in the freezing-tolerant frog Litoria ewingii. *Journal of Comparative Physiology B-Biochemical Systemic and Environmental Physiology*, 181: 781–792.

Ricci, M.A., Bruni, F., Gallo, P., Rovere, M., and Soper, A.K. (2000) Water in confined geometries: experiments and simulations. *Journal of Physics-Condensed Matter*, 12: A345–A350.

Rovere, M. and Gallo, P. (2003) Effects of confinement on static and dynamical properties of water. *European Physical Journal E*, 12: 77–81.

Rovere, M., Ricci, M.A., Vellati, D., and Bruni, F. (1998) A molecular dynamics simulation of water confined in a cylindrical SiO_2 pore. *Journal of Chemical Physics*, 108: 9859–9867.

Rupley, J.A. and Careri, G. (1991) *in Advances in Protein Chemistry*, 41: 37.

Rupley, J.A., Gratton, E., and Careri, G. (1983) Water and Globular-Proteins. *Trends in Biochemical Sciences*, 8: 18–22.

Sartor, G., Mayer, E., and Johari, G.P. (1994) Calorimetric Studies of the Kinetic Unfreezing of Molecular Motions in Hydrated Lysozyme, Hemoglobin, and Myoglobin. *Biophysical Journal*, 66: 249–258.

Sellberg, J.A., Huang, C., McQueen, T.A., Loh, N.D., Laksmono, H., Schlesinger, D., Sierra, R.G., Nordlund, D., Hampton, C.Y., Starodub, D., DePonte, D.P., Beye, M., Chen, C., Martin, A.V., Barty, A., Wikfeldt, K.T., Weiss, T.M., Caronna, C., Feldkamp, J., Skinner, L. B., Seibert, M.M., Messerschmidt, M., Williams, G.J., Boutet, S., Pettersson, L.G.M., Bogan, M.J., and Nilsson, A. (2014) Ultrafast X-ray probing of water structure below the homogeneous ice nucleation temperature. *Nature*, 510: 381–384.

Shamblin, S.L., Tang, X.L., Chang, L.Q., Hancock, B.C., and Pikal, M.J. (1999) Characterization of the time scales of molecular motion in pharmaceutically important glasses. *Journal of Physical Chemistry B*, 103: 4113–4121.

Shibata, Y., Kurita, A., and Kushida, T. (1998) Real-time observation of conformational fluctuations in Zn-substituted myoglobin by time-resolved transient hole-burning spectroscopy. *Biophysical Journal*, 75: 521–527.

Sinibaldi, R., Ortore, M.G., Spinozzi, F., Carsughi, F., Frielinghaus, H., Cinelli, S., Onori, G., and Mariani, P. (2007) Preferential hydration of lysozyme in water/glycerol mixtures: A small-angle neutron scattering study. *Journal of Chemical Physics*, 126: 235101

Sjostrom, J., Mattsson, J., Bergman, R., and Swenson, J. (2011) Hydrogen Bond Induced Nonmonotonic Composition Behavior of the Glass Transition in Aqueous Binary Mixtures. *Journal of Physical Chemistry B*, 115: 10013–10017.

Sjostrom, J., Swenson, J., Bergman, R., and Kittaka, S. (2008) Investigating hydration dependence of dynamics of confined water: Monolayer, hydration water and Maxwell-Wagner processes. *Journal of Chemical Physics*, 128: 154503.

Speedy, R.J. and Angell, C.A. (1976) Isothermal compressibility of supercooled water and evidence for a thermodynamic singularity at −45 degrees C. *Journal of Chemical Physics*, 65: 851–858.

Swenson, J. (2004) The glass transition and fragility of supercooled confined water. *Journal of Physics-Condensed Matter*, 16: S5317–S5327.

Swenson, J. and Cerveny, S. (2015) Dynamics of deeply supercooled interfacial water. *Journal of Physics-Condensed Matter*, 27: 033102.

Swenson, J., Elamin, K., Jansson, H., and Kittaka, S. (2013) Why is there no clear glass transition of confined water? *Chemical Physics*, 424: 20–25.

Swenson, J., Jansson, H., and Bergman, R. (2006) Relaxation processes in supercooled confined water and implications for protein dynamics. *Physical Review Letters*, 96: 247802.

Swenson, J., Jansson, H., Hedstrom, J., and Bergman, R. (2007) Properties of hydration water and its role in protein dynamics. *Journal of Physics-Condensed Matter*, 19: 205109.

Swenson, J. and Teixeira, J. (2010) The glass transition and relaxation behavior of bulk water and a possible relation to confined water. *Journal of Chemical Physics*, 132: 014508.

Takahara, S., Nakano, M., Kittaka, S., Kuroda, Y., Mori, T., Hamano, H., and Yamaguchi, T. (1999) Neutron scattering study on dynamics of water molecules in MCM-41. *Journal of Physical Chemistry B*, 103: 5814–5819.

Tammann, G. and Hesse, W. (1926) The dependancy of viscosity on temperature in hypothermic liquids. *Zeitschrift Fur Anorganische Und Allgemeine Chemie*, 156: 245–257.

Tarek, M. and Tobias, D.J. (2002) Role of protein-water hydrogen bond dynamics in the protein dynamical transition. *Physical Review Letters*, 88: 138101–138104.

Tarek, M. and Tobias, D. J. (2002) Single-particle and collective dynamics of protein hydration water: A molecular dynamics study. *Physical Review Letters*, 89: 275501.

Wang, Z., Fratini, E., Li, M., Le, P., Mamontov, E., Baglioni, P., and Chen, S.-H. (2014) Hydration-dependent dynamic crossover phenomenon in protein hydration water. *Physical Review E*, 90: 042705.

Vitkup, D., Ringe, D., Petsko, G.A., and Karplus, M. (2000) Solvent mobility and the protein 'glass' transition. *Nature Structural Biology*, 7: 34–38.

Vogel, H. (1921) The temperature dependence law of the viscosity of fluids. *Physikalische Zeitschrift*, 22: 645–646.

Vogel, M. (2008) Origins of apparent fragile-to-strong transitions of protein hydration waters. *Physical Review Letters*, 101: 225701–225704.

Yoshida, K., Yamaguchi, T., Kittaka, S., Bellissent-Funel, M.-C., and Fouquet, P. (2008) Thermodynamic, structural, and dynamic properties of supercooled water confined in mesoporous MCM-41 studied with calorimetric, neutron diffraction, and neutron spin echo measurements. *Journal of Chemical Physics*, 129: 054702.

Zimmerman, S.B. and Minton, A.P. (1993) Macromolecular crowding – biochemical, biophysical and physiological consequences. *Annual Review of Biophysics and Biomolecular Structure*, 22: 27–65.